

CFD Based Optimization of Oscillatory Wing Motion for Maximum Energy Harvesting from Wind

Mustafa Kaya*[‡], Munir Elfarra*

* Department of Aeronautical Engineering, Faculty of Aeronautics and Astronautics, Ankara Yildirim Beyazit University, Ankara/Turkey

(mukaya@ybu.edu.tr, melfarra@ybu.edu.tr)

[‡]Corresponding Author; Mustafa Kaya, Ankara Yildirim Beyazit Universitesi Havacilik ve Uzay Bilimleri Fakultesi Cicek Cad. Ulus Ankara Turkey, Tel: +90 312 906 1387,

Fax: +90 312 324 1505, mukaya@ybu.edu.tr

Received: 14.11.2017 Accepted: 17.01.2018

Abstract- Oscillating wing is an innovative approach for power extraction from wind. The parameters which define the oscillatory motion of an airfoil are optimized using the Response Surface Methodology (RSM). The objective of the optimization is to maximize the power extraction from wind. The flows around the oscillating airfoil are computed unsteady and laminar using a Navier-Stokes solver. The computations are conducted parallel in a PC cluster. The oscillatory motion is defined as a combination of plunging and pitching. The optimization variables are the oscillation frequency, the plunge and pitch amplitudes and the phase shift between plunging and pitching. The calculated highest power coefficient is about 0.40, which is comparable to the power coefficient values of conventional rotating wind turbines. The optimum motion is obtained when the reduced frequency is almost unity. Moreover, the maximum power coefficient increases as the plunge amplitude increases.

Keywords Oscillating Wings; Wind Energy; Computational Fluid Dynamics; Optimization; Response Surface Methodology; Parallel Processing.

1. Introduction

Power generation based on the renewable energy sources is a recently spread idea. Extraction of the power from the air/water flow energy is a good example for the renewable energy sources [1-4]. For this purpose, the conventional rotating wind turbines are commonly used for years. Ocean current and water stream flow are also other renewable energy sources [5].

CFD is a common tool for the design and performance analysis of wind turbine blades and wind assessment [4, 6-8].

The non-conventional oscillating wings can be considered as another solution for extracting power from air. Studies on oscillating-wing wind power generators have been started few years ago. McKinney and DeLaurier [9] have analytically and experimentally analyzed the flows over oscillating wings to investigate their ability in producing power from wind energy. Their results have shown that oscillating wings can generate power as efficient as

conventional wind turbines. They have found power coefficient of about 30% at a certain combination of plunging and pitching and a phase shift between plunge and pitch motions. Their results are promising for further investigations.

For a long time after McKinney and DeLaurier's work, studies on oscillating/flapping wings have focused on mostly the thrust generation rather than power generation. Jones et al. [10,11] have conducted two important studies to investigate the usage of oscillating wings to extract power from the wind energy. They have numerically and experimentally investigated a single wing oscillating in the air flow, and dual wings in tandem oscillating in the water flow. The numerical analyses in those studies have been done in two-dimension. They have investigated sinusoidal plunging and pitching motions which give high power coefficients.

Kinsey and Dumas [12] have used a 2-D Navier-Stokes solver to compute the flows over an airfoil undergoing a

combination of sinusoidal plunge and pitch motions. Their parametric study have shown that about 35% power coefficient can be attained. Liu et al. [13] used Discrete Vortex Method to solve the same problem of Kinsey and Dumas [12] to validate their method. They obtained results with 1% deficiency from Kinsey and Dumas.

Kinsey and Dumas [14] have also compared the results of 2-D and 3-D solutions of water flows over oscillating wings. They have observed that generated powers based on 3-D solutions follow a similar trend to the 2-D solutions although 3-D solutions have provided relatively 20% - 30% less power coefficient. However, in the case of using wing end plates, their 3-D solutions have not differed by more than 10% from the 2-D ones. Based on this observation, Kinsey and Dumas [15] have suggested that 2-D solutions which take shorter computation durations can be validated against 3-D solutions using correction factors.

Nonsinusoidal flapping motions of airfoils have been reported to be superior to sinusoidal motions regarding thrust generation [16]. This observation might also be true for power production using oscillating airfoils. Therefore, Platzer et al. [17] have suggested an oscillatory motion based on square waves to increase the power generation. They have also observed from their experiments that wings oscillating in tandem configuration can enhance the power production.

Ashraf et al. [18] have proposed a new oscillating-wing mechanism to generate power from wind and flowing water. Their mechanism is based on nonsinusoidal plunging and pitching. They solved 2-D Navier-Stokes equations for air flows over oscillating airfoils. The results have shown that the power coefficient increases by about 15% compared to an airfoil which makes a sinusoidal plunging and pitching. They have also studied the case of two airfoils in a tandem configuration. According to the cases they have studied and the mechanism they have used, the power coefficient per airfoil is not affected compared to a single oscillating airfoil.

Kinsey and Dumas [15] have focused on the determination of the optimal positioning of dual wings in a tandem configuration oscillating in water flow to obtain the maximum power coefficient. For this purpose, they have used a 2-D Navier-Stokes solver. They have observed that a high power may be obtained if the aft wing is at a proper position.

Zhu et al. [19] have proposed a new adaptive deformation oscillating wing to investigate energy extraction from incoming stream. In their study, they presented the theoretical performance of this concept through unsteady two-dimensional simulations. They have reported that the power coefficient can be increased by around 16% compared to oscillating airfoils which are not undergoing a deformation process.

Young et al. [20] have conducted a review on the progress and challenges of using flapping foils as power generators. They concluded that this field is currently witnessing a rapid increase in research and publications. However, more studies are needed in this area.

In literature, the optimization to examine the optimum oscillating parameters for maximum power production was not conducted. This study aims at determining the oscillatory motion parameters for the maximum generated power coefficient using a numerical optimization method. For this purpose, an airfoil oscillating as a linear combination of sinusoidal plunging and pitching are analyzed numerically. The aerodynamic loads are obtained from 2-D unsteady laminar flow computations. The optimization is based on Response Surface Methodology (RSM). The flow computations are done in a parallel computing environment.

2. Numerical Method

2.1. Navier-Stokes Solver

The unsteady, 2-D, thin-layer, Reynolds averaged Navier-Stokes equations for compressible flows are implicitly solved on a structured grid (Kaya and Tuncer [16, 21]; Kaya et al. [22]). The computations are performed in a parallel computing environment based on domain decomposition (Fig. 1). The oscillatory motion is obtained by the giving the prescribed plunge and pitch motions (equations (1) and (2)) to the airfoil. The C-grid surrounding the airfoil is also moved with the same motions.

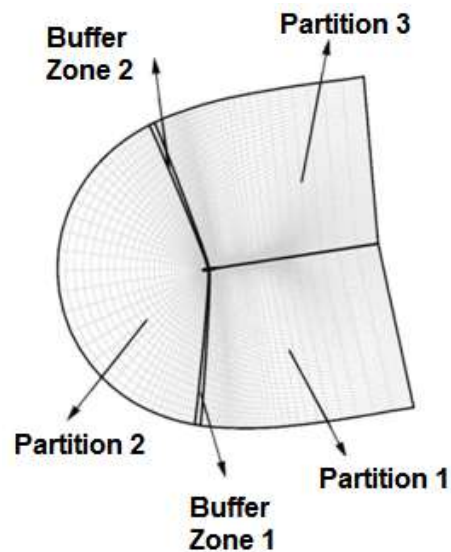


Fig. 1. Grid decomposition.

The non-dimensional Navier-Stokes equations are solved on each grid partition. Boundary conditions for each subgrid are satisfied by interchanging the flow variables on the buffer zones between the partitions. The fluxes are computed using the third order Osher's upwind biased flux difference splitting implicit scheme [23, 24].

2.2. Boundary Conditions

The Navier-Stokes solver is formulated using an inertial frame of reference. Therefore, the prescribed oscillatory motion is assigned as the flow velocity on the airfoil surface on each time step.

The flow variables at the farfield boundaries are calculated using the non-reflecting boundary conditions [25].

The flow variables on the wake cut of the C-grid are computed using Riemann invariants.

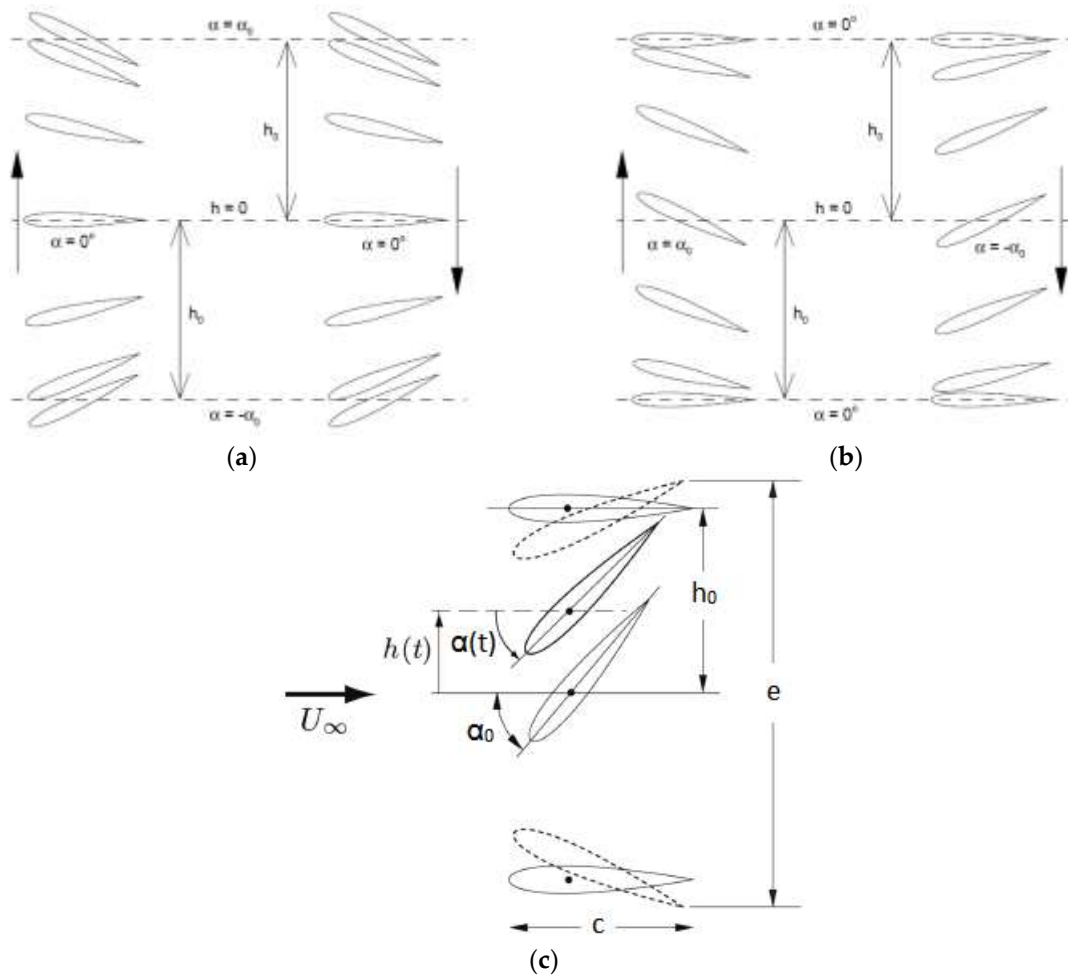


Fig. 2. Oscillation motion as a combination of plunging and pitching: (a) Case of phase shift $\phi = 0^\circ$; (b) Case of phase shift $\phi = 90^\circ$; (c) Oscillatory motion and the flow window

2.3. Oscillatory Motion of the Airfoil

The oscillatory motion is given by sinusoidal plunge, $h(t)$, and sinusoidal pitch, $\alpha(t)$, motions:

$$h = -h_0 \cos(\omega t) \tag{1}$$

$$\alpha = -\alpha_0 \cos(\omega t + \phi) \tag{2}$$

where h_0 and α_0 are the amplitudes of the plunge and pitch motions respectively. The circular frequency is defined as $\omega = 2\pi f$ where f is the oscillation frequency. t is the time and ϕ is the phase shift between plunging and pitching. h and h_0 are non-dimensionalised by the airfoil chord length c .

The motion is shown in Fig. 2. In this figure, e , is the total excursion of the airfoil, that is, the maximum distance in the plunge axis that the airfoil can travel during an oscillation period. e may be also called as the flow window. U_∞ is the freestream velocity. The arrow in the figure shows the flow direction.

In literature, there are various parameters used to investigate the flapping motion of airfoils. Some of them, which are also used in the present work, are the reduced frequency, k , the effective angle of attack, α_{eff} , and the feathering parameter, χ . Those parameters are defined in the equations below:

$$k = \frac{\omega c}{U_\infty} \tag{3}$$

$$\alpha_{eff}(t) = \alpha(t) - \arctan\left(\frac{\dot{h}c}{U_\infty}\right) \tag{4}$$

$$\chi = \frac{\alpha_0}{\arctan(kh_0)} \tag{5}$$

2.4. Evaluation of Power Coefficient

In this study, the non-dimensional power coefficient $C_p^*(t)$ is considered instead of the instantaneous generated power, $P(t)$, during the oscillation. $C_p^*(t)$ is defined in

equation (6). ρ in the equation is the freestream density. The average power coefficient, C_p , obtained in one period is defined in equation (7). $C_l(t)$ and $C_m(t)$ in this equation are the instantaneous lift and moment coefficients respectively. The moment is computed with respect to the pitching center.

As noticed from the equations, an oscillation motion with smaller flow window gives higher power coefficient compared to another motion of the same generated power but with a larger flow window.

$$C_p^*(t) = \frac{P(t)}{1/2 \rho U_\infty^3 c} = C_l(t)\dot{h}(t) + C_m(t)\dot{\alpha}(t)c \quad (6)$$

$$C_p = \frac{1}{e/c} \frac{1}{U_\infty} \int_0^1 (C_l(t)\dot{h}(t) + C_m(t)\dot{\alpha}(t)c) d(t/T) \quad (7)$$

2.5. Optimization

In this study, optimization variables are the motion parameters which define the oscillation. Those parameters are the oscillation frequency, the amplitudes of pitch and plunge motions and the phase shift between them. The objective function is the power coefficient.

The Response Surface Methodology (RSM) is employed for the optimization. RSM is mainly used to construct global approximations to a function based on its values computed at various points [26]. The method is widely used when optimization of a function is expensive and difficult in terms of computational resources.

2.6. Parallel Computation

The parallel computations are conducted on a PC cluster consisting of multi-processor computers running on a 64 bit Linux Operator System. A simple parallel algorithm based on a master-worker paradigm on more than one processor is used for the flow computations. As mentioned before, the computational domain is decomposed into partitions, the solutions on which are computed in different processors in the cluster. The PVM library routines (Parallel Virtual Machine, version 3.4.6) are utilized for the communication between the processors.

3. Solver Validation

The space and time resolution is based on the previous studies [16, 21, 22]. The C-grid (Fig. 1) has 401x201 nodes while there are 10000 time steps per oscillation period. The node distribution near the airfoil surface is fine enough (the first spacing is 1.5×10^{-4} chord length) to catch the boundary layer characteristics according to the input Reynolds number, $Re=1100$. The Navier-Stokes solver and the used time and space resolution are validated against experimental and numerical works done by other researchers.

In the experimental study conducted by Simpson [27] at a Reynolds number of 13,800, a flapping NACA0012 has the following sinusoidal effective angle of attack, α_{eff} :

$$\alpha_{eff}(t) = -\alpha_{eff,o} \cos(\omega t + \phi) \quad (8)$$

where $\alpha_{eff,o}$ is the maximum effective angle of attack during one cycle of flapping motion. The nonsinusoidal plunge motion they have used is therefore defined by:

$$h(t) = \int_0^1 \tan(\alpha(t) - \alpha_{eff}(t)) U_\infty d(t/T) \quad (9)$$

They also have an efficiency definition for power production measure:

$$\eta = \frac{1}{2h_o} \frac{1}{U_\infty} \int_0^1 (C_l(t)\dot{h}(t) + C_m(t)\dot{\alpha}(t)c) d(t/T) \quad (10)$$

This power production efficiency is slightly larger than the power coefficient used in this study as shown in equation (7).

Three cases of low ($h_o = 1.0, \alpha_o = 44.7, k = 0.628$), mid ($h_o = 1.0, \alpha_o = 72.1, k = 0.628$) and high ($h_o = 0.75, \alpha_o = 72.1, k = 0.836$) efficiencies are selected for comparison in order to validate the current Navier-Stokes solver and the used temporal and spatial resolution. The experimental results by Simpson [27] and the computed results are compared in terms of unsteady lift coefficient in Fig. 3.

It is seen from Fig. 3 that the computed time variation of lift coefficient, C_l , along an oscillation period agree well with the experimental data. Note that theoretically expected antisymmetry in C_l between upgoing and downgoing flapping motion is not observed in the experimental results.

The validation is also done against Kinsey and Dumas' numerical work [12]. The power coefficient results are compared with their work in Table 1. As seen, the results of the present work are in a good agreement with the results of Kinsey and Dumas [12].

4. Results and Discussion

In order to comply with the past studies in literature [12,18], the flow solutions are based on the laminar flow assumption. The incompressible nature of the low wind speed is simulated using a low freestream Mach Number in the non-dimensional flow solver used. Again to be consistent with Platzler et al. [17] and Ashraf et al. [18] the freestream Reynolds number is selected as $Re = 1100$. The airfoil used is the NACA0012 profile. Pitching center location on the chord is selected at 1/3 chord length from the leading edge as in Kinsey and Dumas [12] and Simpson [27]. Since the Navier-Stokes equations solved are non-dimensional, the chord length is unity in the solver

All the computations are carried out in a parallel computing environment by decomposing the grid into 3 partitions, each of which is assigned to a separate CPU. Therefore, out of the cases spanning the parametric space,

some are calculated simultaneously since there are 48 available processors in the PC cluster. The computation of a typical unsteady flow solution for the 5-period oscillation motion takes about 15-20 minutes of wall clock time. The power coefficient is calculated using the aerodynamic loads computed during the 5th period.

Parametric space is spanned over a certain range of reduced frequency, k , pitch amplitude, α_0 , plunge amplitude, h_0 , and the phase shift between plunging and pitching, ϕ . k , varies logarithmically in the range between 0.15 – 1.50, where, α_0 , varies linearly in the range 5°-90°. h_0 , and, ϕ , vary linearly in the ranges 0.5-1.5 and 60°-120° respectively. The spanned parametric space is given in Table 2.

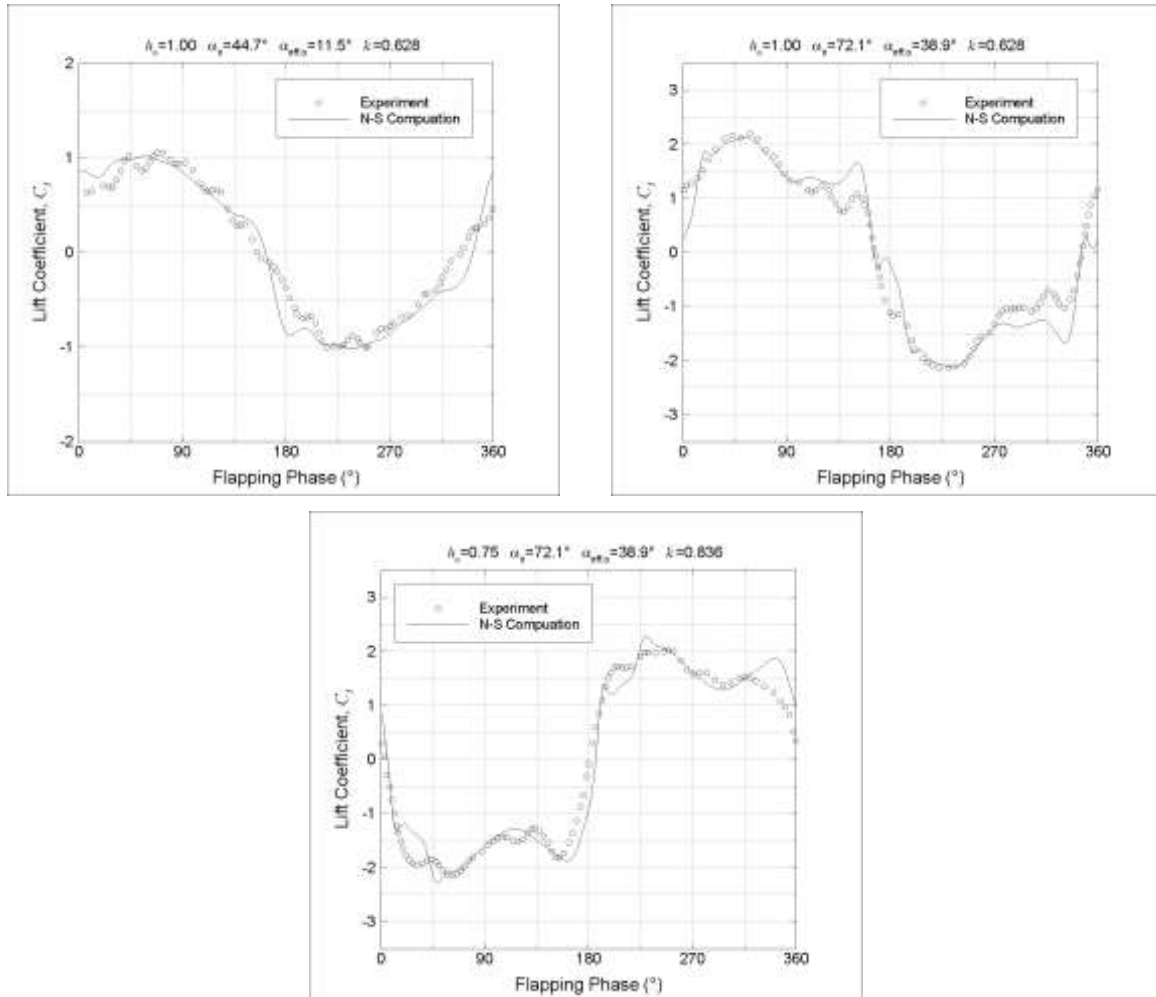


Fig. 3. Comparison of computed unsteady lift coefficient to experimental results.

Table 1. Power coefficient comparison to Kinsey and Dumas [12].

Oscillatory Motion Parameters	Present Work	Kinsey and Dumas' work	Relative Difference (%)
$h_0 = 1.0, k = 0.377, \alpha_0 = 60.0^\circ, \phi = 90^\circ$	0.128	0.123	4.07
$h_0 = 1.0, k = 0.754, \alpha_0 = 60.0^\circ, \phi = 90^\circ$	0.262	0.245	6.94
$h_0 = 1.5, k = 0.754, \alpha_0 = 71.5^\circ, \phi = 90^\circ$	0.278	0.263	5.70
$h_0 = 0.5, k = 0.754, \alpha_0 = 44.0^\circ, \phi = 90^\circ$	0.213	0.208	2.40

Table 2. The parametric space of the oscillatory motion.

		Plunge Amplitude, h_0				
		0.50	0.75	1.00	1.25	1.50
Phase Shift, ϕ ($^\circ$)	120	<p>Reduced Frequency, $k =$ 0.150, 0.194, 0.250, 0.323, 0.417, 0.539, 0.696, 0.899, 1.160, 1.500</p> <p>Pitch Amplitude ($^\circ$), $\alpha_0 =$ 5.0, 10.0, 15.0, 20.0, 25.0, 30.0, 35.0, 40.0, 45.0, 50.0, 55.0, 60.0, 65.0, 70.0, 75.0, 80.0, 85.0, 90.0</p>				
	105					
	90					
	75					
	60					

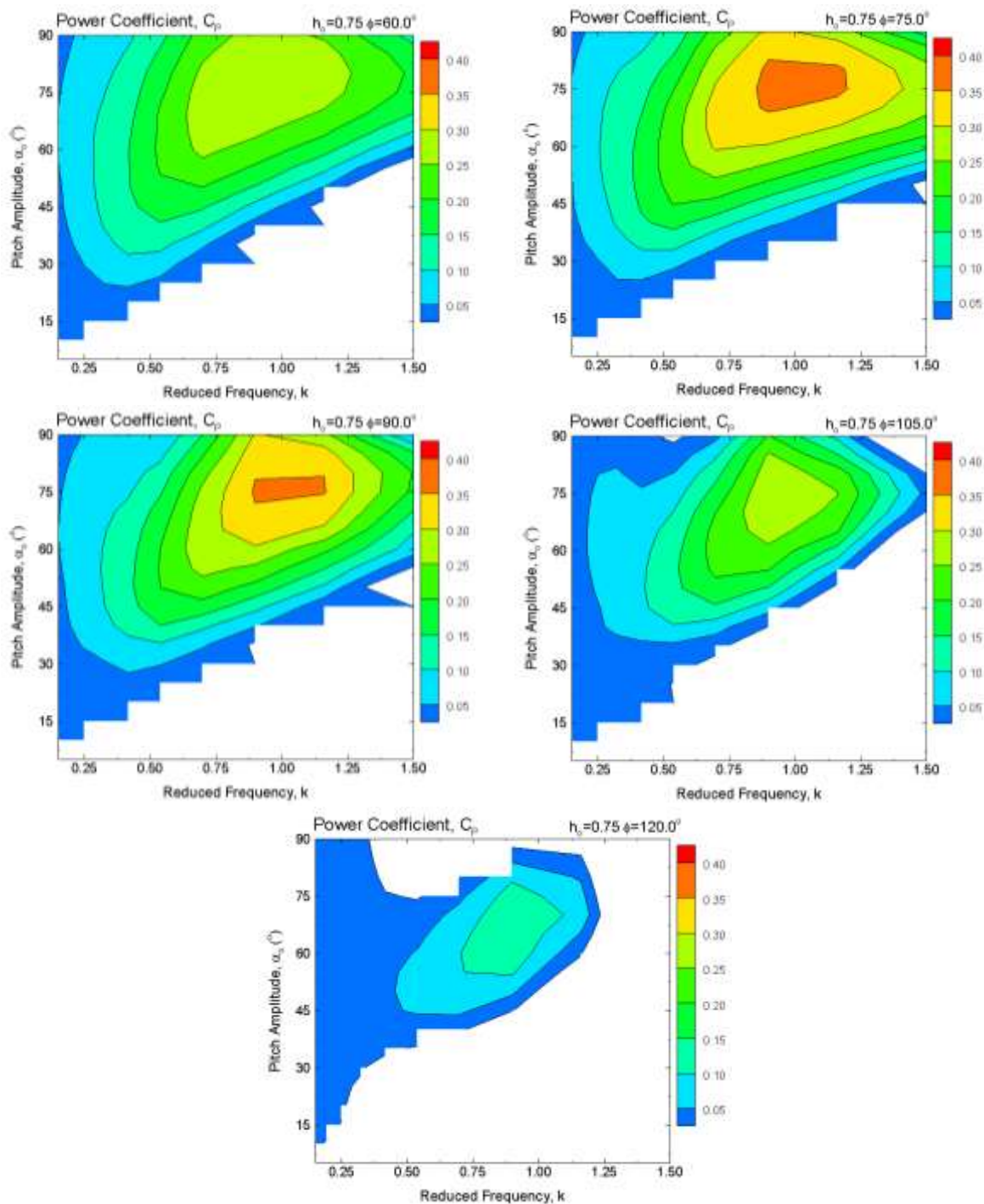


Fig. 4. Power coefficient maps in the, $k - \alpha_0$, parametric space for, $h_0 = 0.75$ case.

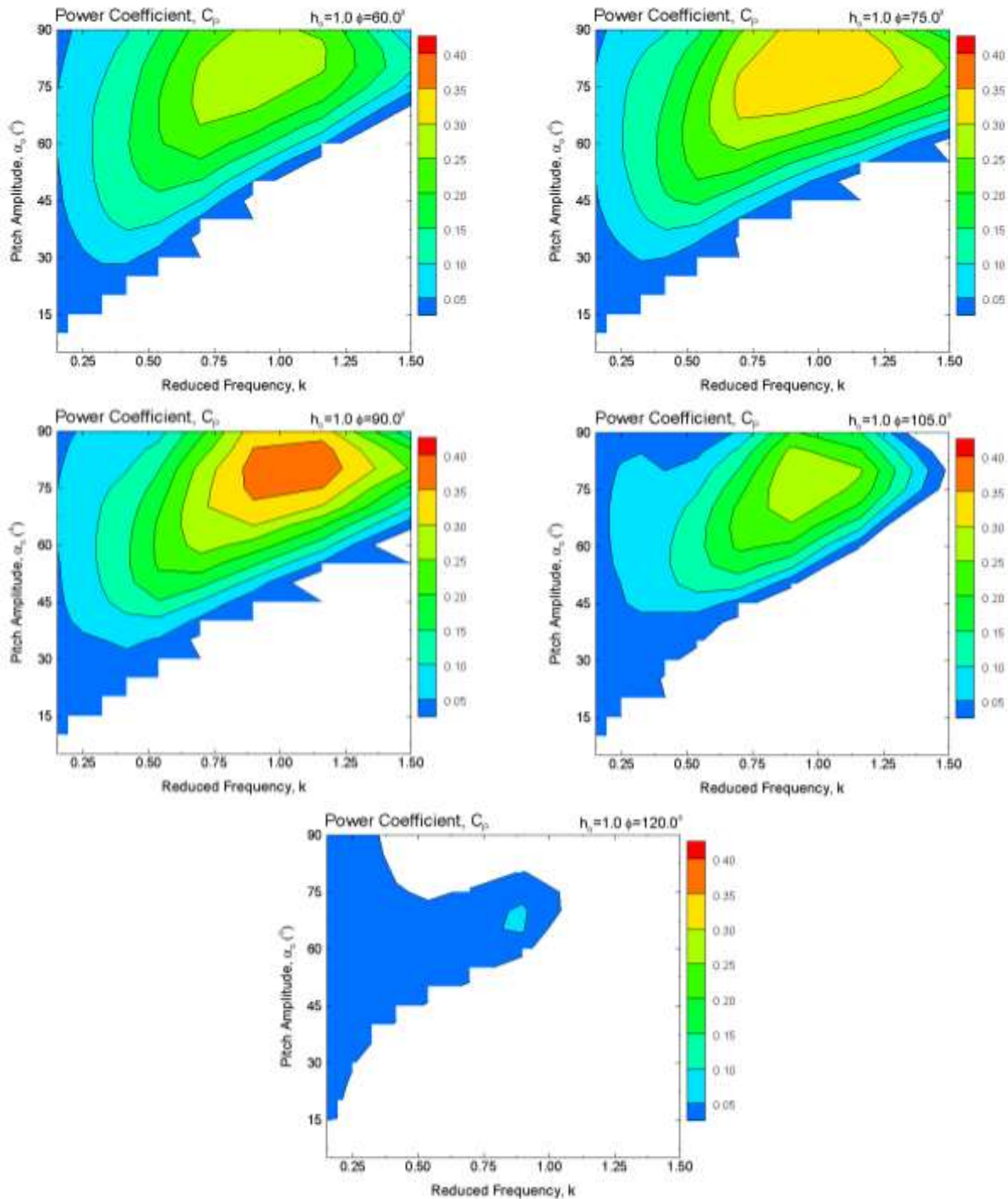


Fig. 5. Power coefficient maps in the, $k - \alpha_0$, parametric space for, $h_0 = 1.00$ case.

In the spanned space there are $5 \times 5 \times 10 \times 18 = 4500$ elements which results 4500 cases to be solved. However, since only the cases which satisfy $\chi > 1$ condition will be taken into account [12], the number of cases to be solved reduces to 3235 since 1265 cases don't satisfy the, $\chi > 1$, condition.

The maps of the calculated power coefficients at fixed, h_0 , and, ϕ , values are obtained in the, $k - \alpha_0$, parametric space. It is noticed that the power coefficient will be

maximum when h_0 is in the range 0.75-1.25 and when ϕ is close to 90° . The maps for $h_0 = 0.75, 1.00$ and 1.25 are plotted in Figures 4-6. Only the power producing cases (positive power coefficient cases) are shown in the figures.

From the maps, it is seen that, for any plunge amplitude and phase shift, the maximum power coefficient is observed when k , and, α_0 , fall in the ranges $0.9 - 1.2$ and $75^\circ - 85^\circ$ respectively.

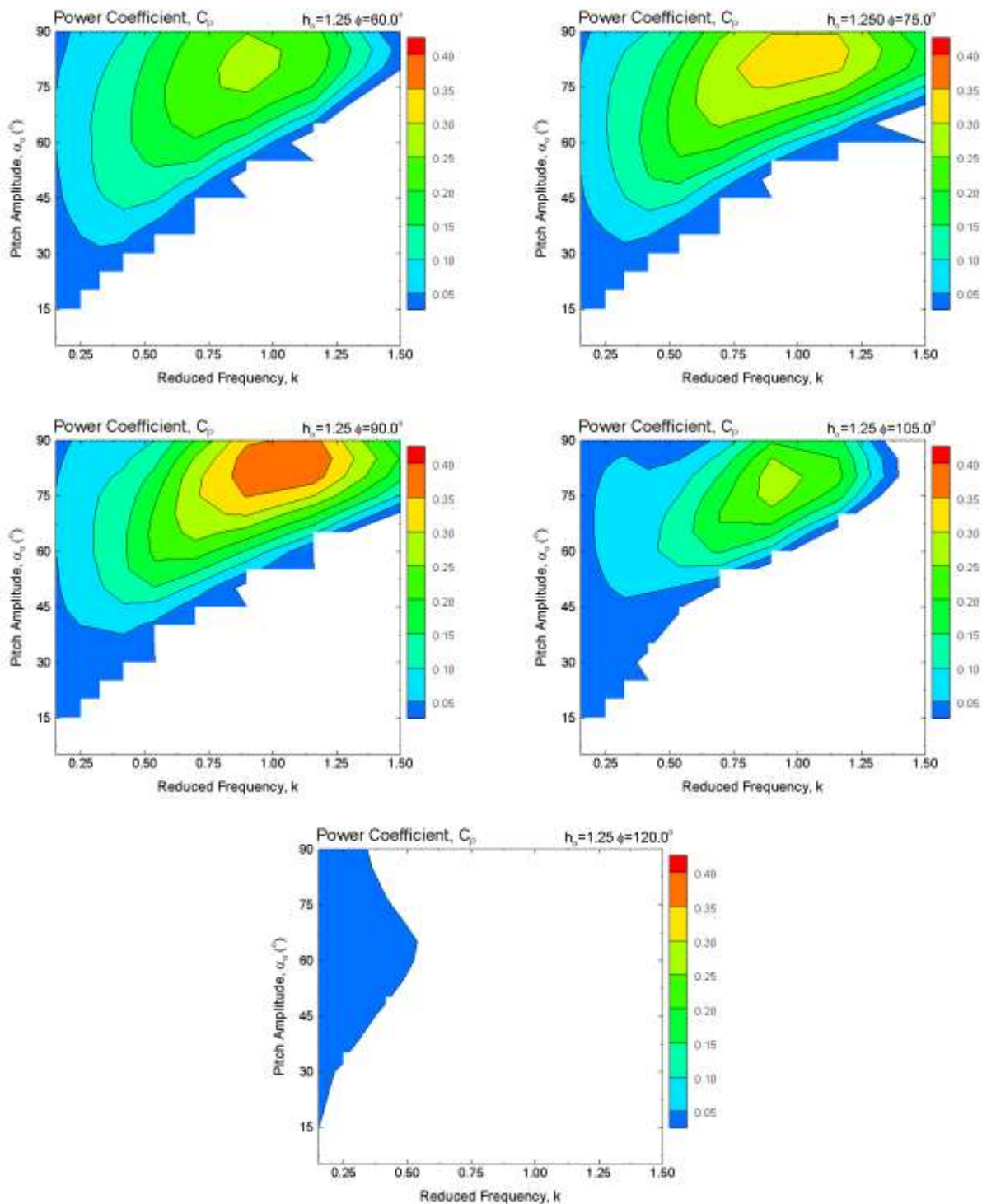


Fig. 6. Power coefficient maps in the, $k - \alpha_0$, parametric space for, $h_0 = 1.25$ case.

The optimum power coefficient is obtained by transforming the maps into response surfaces. For this purpose, a 2nd degree polynomial response surface is produced at fixed, h_0 , and, ϕ , values. The response surface for $h_0 = 1.00$ is shown in Fig. 7. The dots in the figure are

the Navier-Stokes calculations. As seen from the plots, the generated 2nd order polynomial response surfaces approximate the calculated values very well. The maximum residual error is less than 10^{-3} .

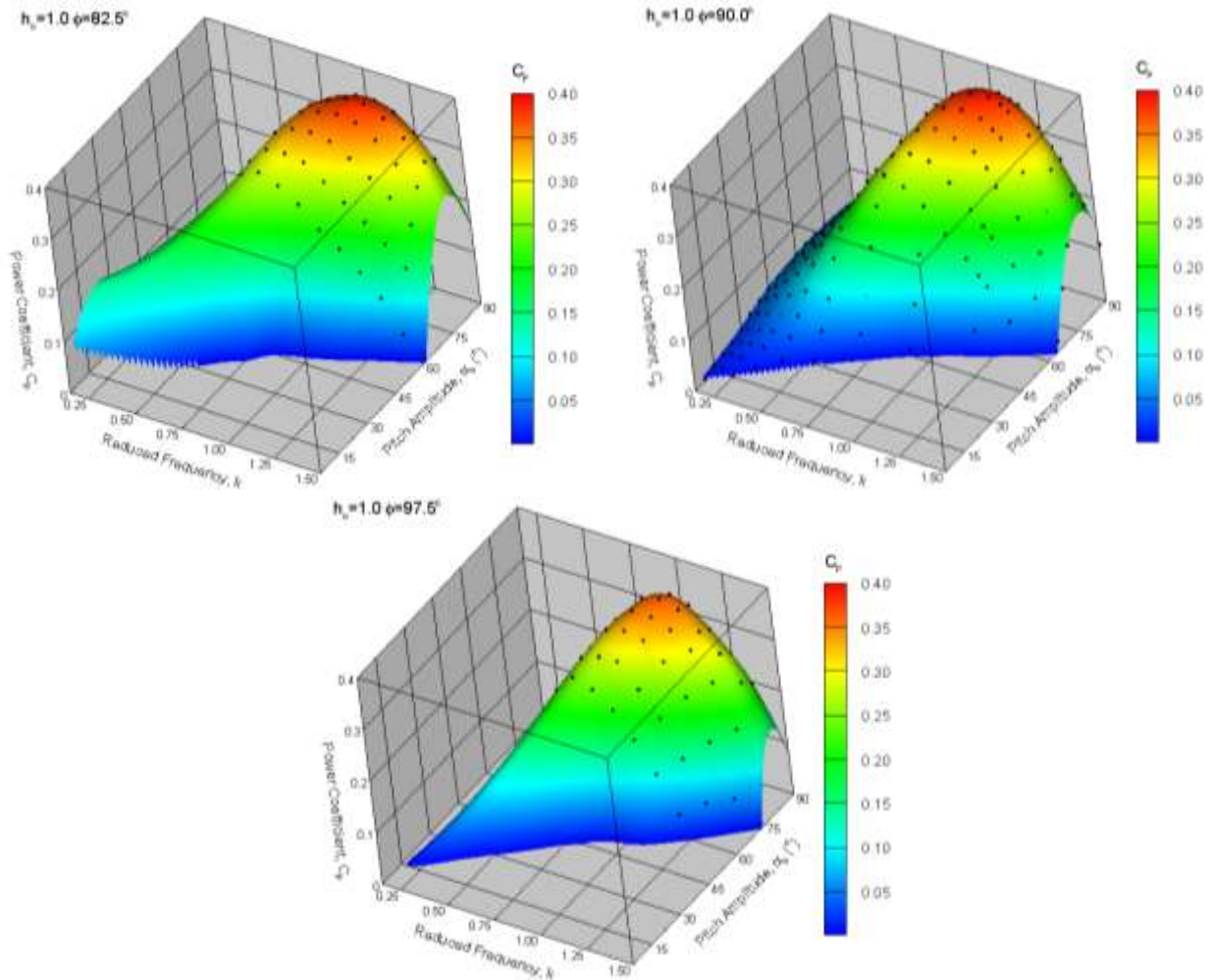


Fig. 7. Power coefficient response surfaces for, $h_0 = 1.0$ case (calculated values are shown in •).

The maximum values of the 2nd degree polynomial response surfaces are computed for varying phase shift values at a fixed value of plunge amplitude. The calculated maximum, C_p , values and the corresponding $k - \alpha_0$ pairs are shown in Figures 8-12. These plots show how the maximum values vary with the phase shift at fixed plunge amplitudes. In the plots, the response surfaces results are also compared to the results calculated by Navier-Stokes to check the accuracy of the response surfaces.

It is observed from the figures that maximum power coefficients for each plunge amplitude, h_0 , occur when the reduced frequency is about $k \sim 1$ as reported by Zhu [28]. Taking into consideration that two trailing edge vortices are generated during the whole oscillation period, and assuming that the advection speed of these vortices is almost same as the freestream speed, then, one can say that the wave number of the vortex shedding of an optimum motion to give

maximum power coefficient is almost equal to the inverse of the half chord length. Zhu [28] relates this frequency to the most unstable mode of the wake. It is interesting that this result is independent of the flow window height (the parameter e in Fig. 2c.).

It is also observed that, for low h_0 values, the maximum power coefficient is obtained when $\phi < 90^\circ$ (between $75^\circ - 90^\circ$) (Figures 8 and 9). On the other hand, for high h_0 values, the maximum C_p value is obtained when $\phi = 90^\circ$ (Figures 10-12). Most probably, the reason is because of the definition of power coefficient given in equation (7). It appears that the most efficient oscillatory motion occurs when the area swept by the airfoil is small.

Another observation is the fact that as the plunge amplitude increases, the pitch amplitude for the maximum power coefficient also increases.

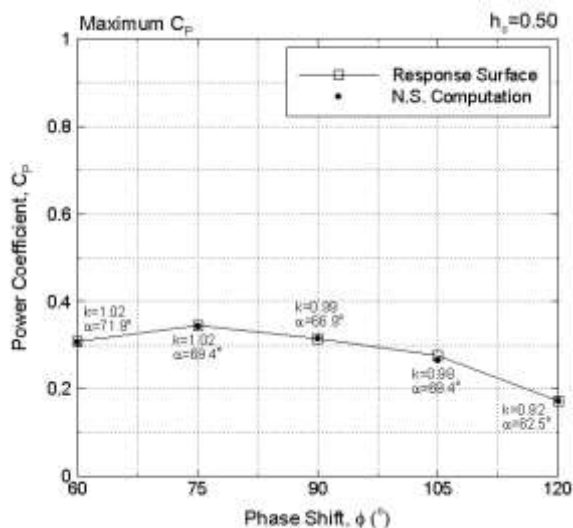


Fig. 8. The maximum power coefficients for $h_0 = 0.50$ case.

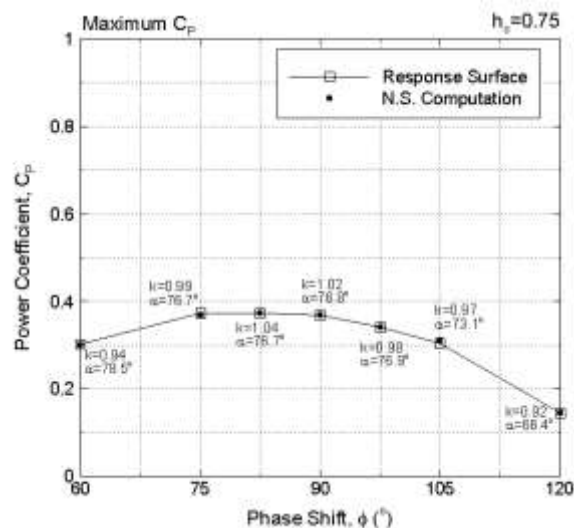


Fig. 9. The maximum power coefficients for $h_0 = 0.75$ case.

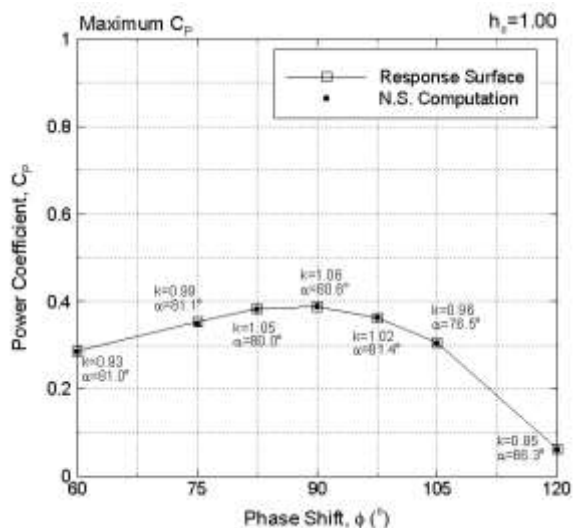


Fig. 10. The maximum power coefficients for $h_0 = 1.00$ case.

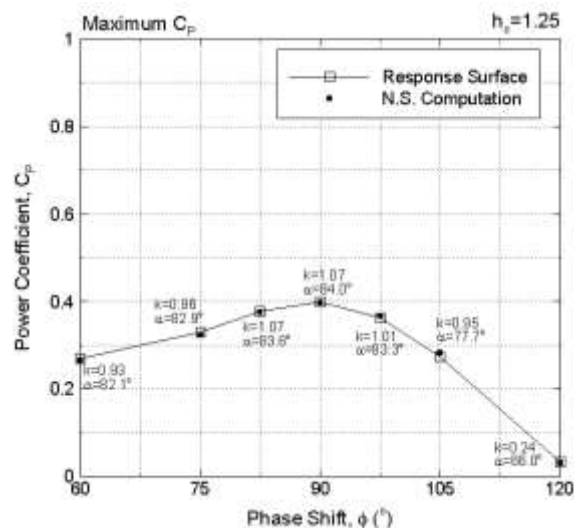


Fig. 11. The maximum power coefficients for $h_0 = 1.25$ case.

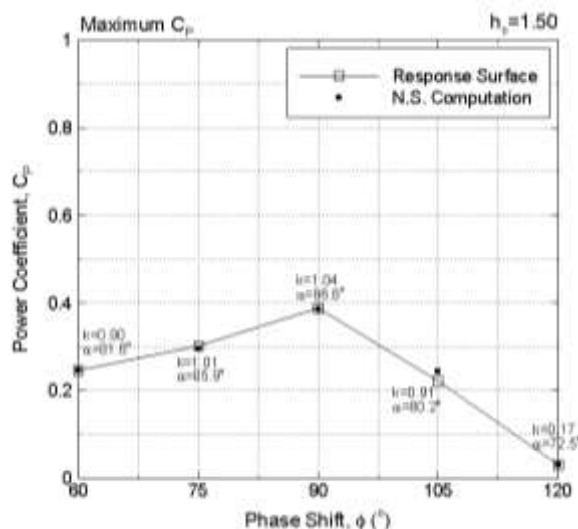


Fig. 12. The maximum power coefficients for $h_0 = 1.50$ case.

Table 3. The highest maximum power coefficient values according to the phase shift.

h_o	$h_o = 0.50$	$h_o = 0.75$	$h_o = 1.00$	$h_o = 1.25$	$h_o = 1.50$
C_p	0.343	0.374	0.389	0.396	0.386
$\begin{pmatrix} \phi \\ k \\ \alpha_o \end{pmatrix}$	$\begin{pmatrix} \phi = 75^\circ \\ k = 1.02 \\ \alpha_o = 69.4^\circ \end{pmatrix}$	$\begin{pmatrix} \phi = 82.5^\circ \\ k = 1.04 \\ \alpha_o = 76.7^\circ \end{pmatrix}$	$\begin{pmatrix} \phi = 90^\circ \\ k = 1.06 \\ \alpha_o = 80.6^\circ \end{pmatrix}$	$\begin{pmatrix} \phi = 90^\circ \\ k = 1.07 \\ \alpha_o = 84.0^\circ \end{pmatrix}$	$\begin{pmatrix} \phi = 90^\circ \\ k = 1.04 \\ \alpha_o = 86.8^\circ \end{pmatrix}$

5. Conclusion

The highest power coefficient is calculated as $C_p = 0.40$. This value is achieved when the plunge amplitude is $h_o = 1.25$. The power coefficient is limited to $C_p = 0.59$ according to Betz’s analysis based on the actuator disk theory [29]. Comparing to Betz’s limit, the result obtained in the current study (maximum power coefficient as $C_p = 0.40$) encourages the further research on oscillating wings to extract power from wind energy. In practice, a power coefficient value above 0.30 may be considered as an alternative and innovative solution for wind power production [12].

The results show that for any plunge amplitude, the maximum power coefficient is obtained when the reduced frequency is about $k \sim 1$ and the phase shift is, $\phi = 90^\circ$.

Acknowledgements

The authors would express their gratitude and thanks to TÜBİTAK (The Science and Technology Research Council of Turkey) for funding support of this work under the 1001 project number 112M933.

References

[1] D. S. Semerci and T. Yavuz, “Increasing Efficiency of an Existing Francis Turbine by Rehabilitation Process”, 5th International Conference on Renewable Energy Research and Applications, Birmingham, UK, 20-23 Nov. 2016. (Conference Paper)

[2] A. Benzerdjeb, B. Abed, H. Achache, M. K. Hamidou, M. Bordjane and A. M. Gorlov, “Numerical Study on the Performance of Darrieus Turbine by k-ε Standard and k-ε EARSM Turbulence Models”, 6th International Conference on Renewable Energy Research and Applications, San Diego, CA, USA, 5-8 Nov. 2017. (Conference Paper)

[3] R. D. Mikhail and S. C. Daniel, “CFD Study of a Vertical Axis Counter-Rotating Wind Turbine”, 6th International Conference on Renewable Energy Research and Applications, San Diego, CA, USA, 5-8 Nov. 2017. (Conference Paper)

[4] I. Colak, M. S. Ayaz and K. Boran, “CFD Based Wind Assessment in West of Turkey”, 4th International

Conference on Renewable Energy Research and Applications, Palermo, Italy, 22-25 Nov. 2015. (Conference Paper)

[5] T. Honda, K. Kasamura, Y. Nakashima, Y. Nakanishi and H. Higaki, “An Ideal Generation System for Streamflow, Tidal and Ocean Currents”, 4th International Conference on Renewable Energy Research and Applications, Palermo, Italy, 22-25 Nov. 2015. (Conference Paper)

[6] E. Anjuri VSJ, “Comparison of Experimental results with CFD for NREL Phase VI Rotor with Tip Plate”, International Journal Of Renewable Energy Research (IJRER), Vol. 2, No. 4, 2012. (Article Paper)

[7] M. M. Yelmule and E. Anjuri VSJ, “CFD predictions of NREL Phase VI Rotor Experiments in NASA/AMES Wind tunnel”, International Journal Of Renewable Energy Research (IJRER), Vol. 3, No. 2, 2013. (Article Paper)

[8] Y. C. Ceballos, M. C. Valencia, D. H. Zuluaga, J. S. Del Rio and S. V. García, “Influence of the Number of Blades in the Power Generated by a Michell Banki Turbine”, International Journal Of Renewable Energy Research (IJRER), Vol. 7, No. 4, 2017. (Article Paper)

[9] W. McKinney, J. DeLaurier, “The Wingmill: An Oscillating-Wing Windmill”, J. Energy, DOI:10.2514/3.6251, Vol. 5, pp. 109-115, 1981. (Article)

[10] K. D. Jones, S. Davids and M. F. Platzer, “Oscillatory-Wing Power Generator”, Proceedings of the 3rd ASME/JSME Joint Fluids Engineering Conference, FEDM’99, San Francisco, California, USA, 1999. (Conference Paper)

[11] K. D. Jones, K. Lindsey and M. F. Platzer, “An Investigation of the Fluid-Structure Interaction in an Oscillating-Wing Micro-Hydropower Generator”, Fluid Structure Interaction 2, Southampton, England, U.K., pp. 73-82, 2003. (Conference Paper)

[12] T. Kinsey and G. Dumas, “Parametric Study of an Oscillating Airfoil in a Power-Extraction Regime”, AIAA J., DOI: 10.2514/1.26253, Vol. 46, pp. 1318-1330, 2008. (Article)

- [13] Z. Liu, J. C. S. Lai, J. Young and F. B. Tian, "Discrete Vortex Method with Flow Separation Corrections for Flapping-Foil Power Generators", AIAA J., DOI: 10.2514/1.J055267, Vol. 55, pp. 410-418, 2017. (Article)
- [14] T. Kinsey and G. Dumas, "Optimal Tandem Configuration for Oscillatory-foils Hydrokinetic Turbine", J. Fluids Eng, DOI: 10.1115/1.4005423, Vol. 134(3), 2012. (Article)
- [15] T. Kinsey and G. Dumas, "Three-dimensional effects on an Oscillating-foils hydrokinetic turbine", J. Fluids Eng, DOI: 10.1115/1.4006914, Vol. 134(7), 2012. (Article)
- [16] M. Kaya and I. H. Tuncer, "Nonsinusoidal Path Optimization of a Flapping Airfoil", AIAA J., DOI: 10.2514/1.29478, Vol. 45, pp. 2075-2082, 2007. (Article)
- [17] M. F. Platzer, M. A. Ashraf, J. Young and J. C. S. Lai, "Extracting Power in Jet Streams: Pushing the Performance of Flapping Wing Technology", 27th Congress of the International Council of the Aeronautical Sciences, International Council of the Aeronautical Sciences Paper 2010-2.9.1, Nice, France, 19-24 Sept. 2010. (Conference Paper)
- [18] M. A. Ashraf, J. Young, J. C. S. Lai and M. F. Platzer, "Numerical Analysis of an Oscillating-Wing Wind and Hydropower Generator", AIAA J., DOI: 10.2514/1.J050577, Vol. 49, pp. 1374-1386, 2011. (Article)
- [19] B. Zhu, W. Han, X. Sun, Y. Wang, Y. Cao, G. Wu, D. Huang and Z. C. Zheng, "Research on energy extraction characteristics of an adaptive deformation oscillating-wing", J Renew Sustain Ener, DOI: 10.1063/1.4913957, Vol. 7, 2015. (Article)
- [20] J. Young, J. C. S. Lai and M. F. Platzer, "A review of Progress and Challenges in Flapping Foil Power Generation", Prog Aerosp Sci, DOI: 10.1016/j.paerosci.2013.11.001, Vol. 67, pp. 2-28, 2017. (Article)
- [21] M. Kaya and I. H. Tuncer, "Path Optimization of Thrust Producing Flapping Airfoils Using Response Surface Methodology", 5th European Congress on Computational Methods in Applied Sciences and Engineering. Venice, Italy, June 30 -July 5, 2008. (Conference Paper)
- [22] M. Kaya, I. H. Tuncer, K. D. Jones and M. F. Platzer, "Optimization of Flapping Motion Parameters for Two Airfoils in a Biplane Configuration", J Aircraft, DOI: 10.2514/1.38796, Vol. 46, pp. 583-592, 2009. (Article)
- [23] S. Osher and S. R. Chakravarty, "A New Class of High Accuracy TVD Schemes for Hyperbolic Conservation Laws", AIAA Paper, No. 85-0363, Aerospace Sciences Meeting, 23rd, Reno, NV, Jan. 14-17, 1985. (Conference Paper)
- [24] S. R. Chakravarty and S. Osher, "Numerical Experiments with the Osher Upwind Scheme For the Euler Equations", AIAA J., DOI: 10.2514/3.60143, Vol. 21, pp. 1241-1248, 1983. (Article)
- [25] M. B. Giles, "Nonreflecting Boundary Conditions for Euler Equation Calculations", AIAA J., DOI: 10.2514/3.10521, Vol. 28, pp. 2050-2058, 1990. (Article)
- [26] W. J. Roux, N. Stander and R. T. Haftka, "Response Surface Approximations for Structural Optimization", Int J Numer Meth Eng, DOI: 10.1002/(SICI)1097-0207(19980615)42:3<517::AID-NME370>3.0.CO;2-L, Vol. 42, pp. 517-534, 1998. (Article)
- [27] B. J. Simpson, Experimental Studies of Flapping Foils for Energy Extraction, MSc thesis, MIT, 2009. (Dissertation)
- [28] Q. Zhu, "Optimal frequency for flow energy harvesting of a flapping foil", J Fluid Mech, DOI: 10.1017/S0022112011000334, Vol. 675, pp. 495-517, 2011. (Article)
- [29] A. Betz, "Das Maximum der Theoretisch Möglichen Ausnützung des Windes Durch Windmotoren", Zeitschrift für das Gesamte Turbinenwesen, Vol. 26, pp. 307-309, 1920. (Article)